Available online at www.sciencedirect.com
SCIENCE DIRECT
Journal of Electroanalytical Chemistry 588 (2006) 88–98
Journal of Electroanalytical Chemistry
www.elsevier.com/locate/jelechem

The effect of hydrogen codeposition on the morphology of copper electrodeposits. I. The concept of effective overpotential

N.D. Nikolić [a,*], K.I. Popov [b], Lj.J. Pavlović [a], M.G. Pavlović [a]

[a] *ICTM – Institute of Electrochemistry, University of Belgrade, Department of Electrochemistry, Njegoševa 12, P.O. Box 473, 11001 Belgrade, Serbia and Montenegro*

[b] *Faculty of Technology and Metallurgy, University of Belgrade, Karnegijeva 4, P.O. Box 3503, 11001 Belgrade, Serbia and Montenegro*

Received 14 July 2005; received in revised form 7 December 2005; accepted 7 December 2005

Abstract

The effect of hydrogen codeposition on the morphology of copper electrodeposits was studied. The dependences of the overall current and the volume of evolved hydrogen on the quantity of electricity used were plotted and the average current efficiencies of the evolved hydrogen were derived from them. The morphologies of copper electrodeposits were correlated with the hydrogen evolution rates. It was shown that dendrites are the main characteristic of deposits obtained at overpotentials belonging to the limiting diffusion current density plateau, at which the hydrogen evolution rate is low. At larger overpotentials the dominant form become craters in the honeycomb-like electrodeposits due to the intensive hydrogen codeposition.

Keywords: Electrodeposition; Copper; Hydrogen evolution; Morphology; SEM

1. Introduction

The morphology of copper electrodeposits obtained from acid copper sulphate solutions was widely investigated [1,2]. It was shown that in the region of overpotentials corresponding to the activation control of deposition process (approximately up to 100 mV for copper electrodeposition from acid sulphate solutions), the grains with well defined crystal planes are formed. The mixed activation–diffusion controlled electrodeposition (the range of overpotentials between 100 and 300 mV, approximately) produces different growing forms as carrot- and cauliflower-like ones. Dendrites grew in the range of overpotentials between approximately 300 and 750 mV, i.e., at overpotentials corresponding to the plateau of the limiting diffusion current density. At the end of this plateau, the hydrogen codeposition takes place.

The morphology of electrodeposited copper in the presence of hydrogen evolution was described recently, but the mechanism of the formation of this type morphology was not established [3]. The topic of this paper is to do it.

2. Experimental

Copper was potentiostatically deposited from 0.15 M $CuSO_4$ in 0.50 M H_2SO_4, in an open cell, and at a room temperature of (18.0 ± 1.0 °C). Doubly distilled water and analytical grade chemicals were used for the preparation of the solution for the electrodeposition of copper. Reference and counter electrodes were of a pure copper. The electrodepositions of copper were performed at overpotentials of 450, 550, 700, 800 and 1000 mV, respectively, onto cylindrical copper electrodes which formation is described in Refs. [4,5]. The following quantities of electricity for electrodeposition were used: 2.5, 5.0, 10.0 and 20.0 mAh cm^{-2}, respectively.

* Corresponding author. Tel./fax: +381 11 337 03 89.
E-mail address: nnikolic@tmf.bg.ac.yu (N.D. Nikolić).

0022-0728/$ - see front matter © 2005 Elsevier B.V. All rights reserved.
doi:10.1016/j.jelechem.2005.12.006

The copper deposits were examined by the scanning electron microscopy (SEM) – with the use of JOEL T20 instrument.

The procedure for the determination of the average current efficiency of the hydrogen evolution will be given in Appendix A.

3. Results and discussion

The polarisation curve for copper electrodeposition is shown in Fig. 1. Figs. 2 and 3 show the dependences of the overall current and the volume of evolved hydrogen on the time of copper electrodeposition, for deposition overpotentials of 550, 700, 800 and 1000 mV, respectively.

The average current efficiences for hydrogen evolution reaction, derived from diagrams shown in Figs. 2 and 3, are plotted as the function of the quantity of used electricity and presented in Fig. 4(a). The dependence of the average current efficiences on overpotentials of the copper electrodeposition is shown in Fig. 4(b). It is obvious from Fig. 4(a) that the hydrogen codeposition at 700 mV is very small, and that at lower overpotentials it even cannot be observed. The average current efficiency for the hydrogen evolution at overpotential of 800 mV was 10.80%, while at overpotential of 1000 mV was 30.0%. The critical overpotential for the beginning of the hydrogen evolution can be estimated to be about 680 mV from Fig. 4(b). Fig. 4(b) is derived from the data from Fig. 4(a).

The morphologies of copper electrodeposits obtained in different hydrogen codeposition conditions are shown in Figs. 5–15.

The deposits obtained at an overpotential of 550 mV with different quantities of electricity are shown in Figs. 5–7. At this overpotential, there is not a hydrogen codeposition at all. The deposits obtained with a quantity of electricity of 2.5 mAh cm^{-2} are shown in Fig. 5(a) and (b). The surface film is completed, the grains grown by electrodeposition on the initially formed nuclei practically touch each other, and there is not a new nucleation on already existing grains. The difference in size between grains can also be observed. This is due to the fact that the nucleation does not occur simultaneously over the whole cathode surface, but it is a process extended in time, so that crystals generated earlier may be considerably larger in the size than ones generated later. These differences increase with an increased quantity of electrodeposited metal, which can be seen from Fig. 6(a) and (b) presenting copper deposits obtained with a quantity of electricity of 5.0 mAh cm^{-2}. These enlarged differences are also the consequence of the fact that some smaller grains are consumed by the larger ones [6], as can be deduced from Figs. 5 and 6(a). This is also illustrated by Fig. 7(a) and (b). The increase of the quantity of the electrodeposited metal led to the formation of a cauliflower structure (Fig. 7(b)). Furthermore, from

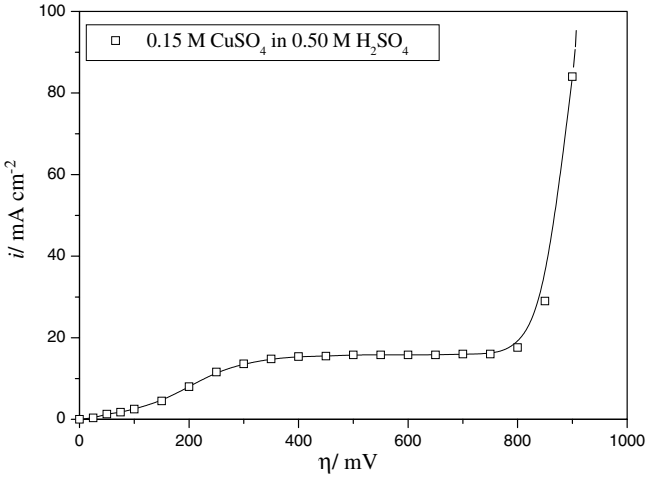

Fig. 1. Polarisation curve for the cathodic process of copper deposition from 0.15 M $CuSO_4$ in 0.50 M H_2SO_4.

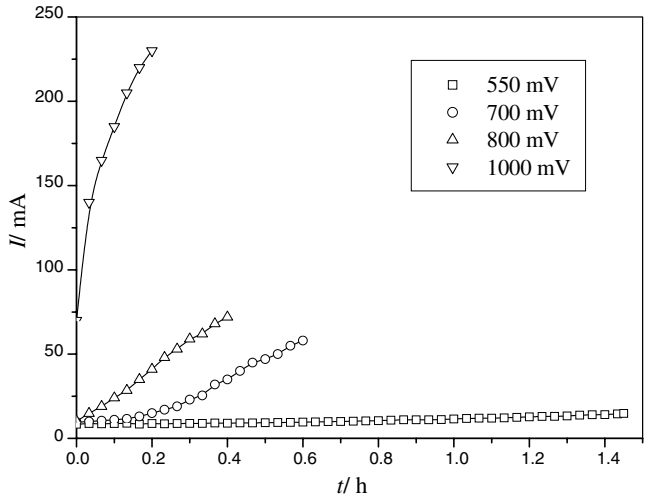

Fig. 2. The dependence of the current of copper electrodeposition on the time of copper electrodeposition, for the copper electrodepositions at 550, 700, 800 and 1000 mV.

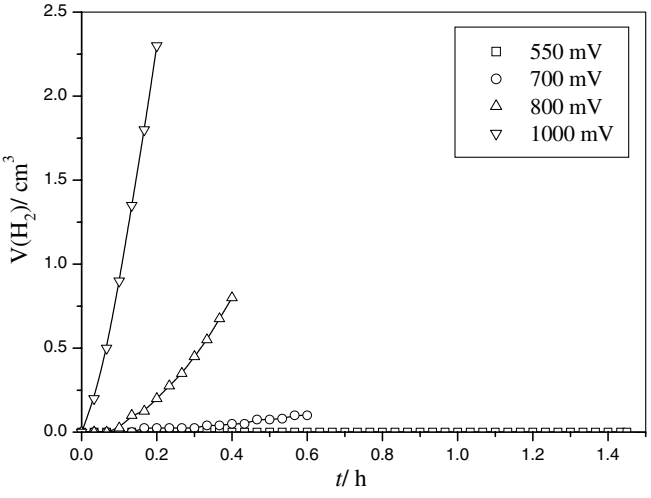

Fig. 3. The dependence of the volume of the evolved hydrogen on the time of copper electrodeposition, for the copper electrodepositions at 550, 700, 800 and 1000 mV.

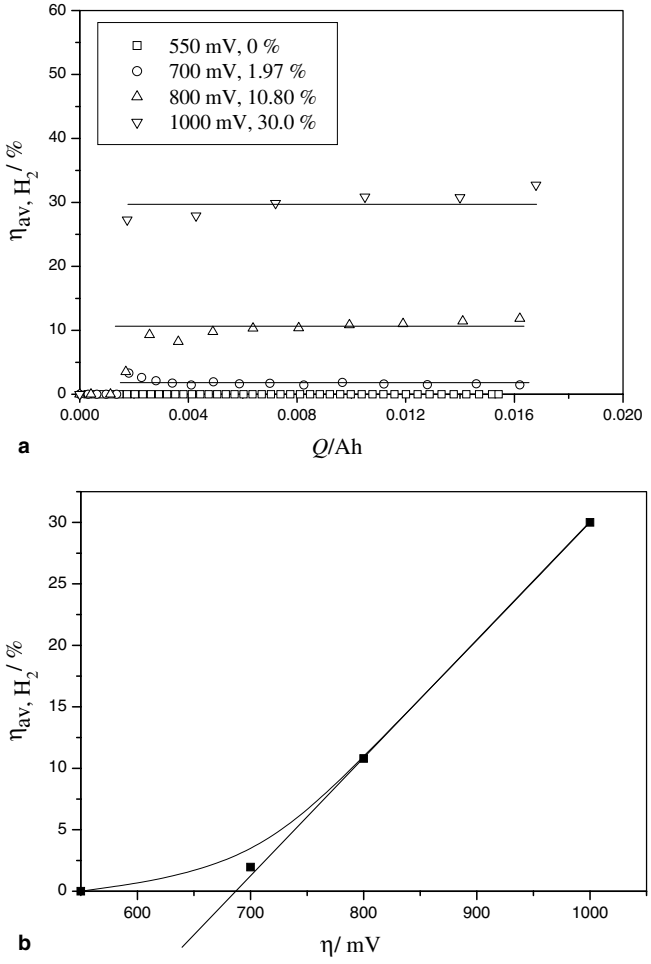

Fig. 4. (a) The dependence of the average current efficiencies for hydrogen evolution reaction on the quantity of an used electricity, for the copper electrodepositions at 550, 700, 800 and 1000 mV. (b) The dependence of the average current efficiencies on overpotentials of the copper electrodeposition.

Fig. 7(b) can be seen that the spherical diffusion layers inside linear diffusion layer of the macroelectrode are formed around these cauliflower particles. Finally, from Fig. 7(c) presenting copper grains obtained at this overpotential can be noticed that a new nucleation on the enlarged grains becomes possible.

On the other hand, it is well known that the induction time of dendrite growth initiation strongly decreases with increasing overpotential of electrodeposition [7]. The situation on the electrode surface after deposition with 2.5 mAh cm^{-2} at 700 mV (Fig. 8) is very similar to the situation after 10 mAh cm^{-2} at 550 mV (Fig. 7). The most important difference is in the shape and size of growing grains, being less globular and smaller in electrodeposition at 700 mV. Besides, the interparticle distances are relatively equal what indicate that these distances are not due to appearance of hydrogen codeposition which is still very small at 700 mV. Dendrites appear at 700 mV after deposition with 5.0 mAh cm^{-2} (Fig. 9) and practically all surface is covered with them after 10 mAh cm^{-2} (Fig. 10), due to further growth of dendrite precursors shown in Fig. 9(b).

However, cauliflower structures were final copper morphologies obtained at the overpotential of 550 mV with the quantity of the electricity of 10 mAh cm^{-2} (Fig. 7(b)), while dendritic forms were final copper morphologies obtained at the overpotential of 700 mV with the same quantity of the electricity (Fig. 10). As mentioned earlier, at these overpotentials, the hydrogen evolution was zero (at 550 mV) or very small (at 700 mV).

The morphology of copper deposit obtained at overpotential of 800 mV with the quantity of the electricity of 2.5 mAh cm^{-2} (Fig. 11) was similar to morphologies of copper deposits obtained at 550 mV with the quantity of the electricity of 10 mAh cm^{-2} (Fig. 7(a)) and at 700 mV with the quantity of the electricity of 2.5 mAh cm^{-2} (Fig. 8(a)).

Meanwhile, the electrodeposition at 800 mV with the quantity of the electricity of 5.0 mAh cm^{-2} (Fig. 12) did not lead to the formation of copper dendrites as at previously analysed overpotential of 700 mV. The agglomerates of small copper grains become dominant form of the copper morphology electrodeposited at this overpotential (Fig. 12(a)). Also, there are large holes or craters between the agglomerates of these grains, which is probably due to the hydrogen codeposition (Fig. 12(b) and (c)). This copper deposit is denoted as a honeycomb-like with craters as main characteristic. In this way, morphologies of copper and tin deposits given in Ref. [3] can be explained. The same morphology of copper deposit remained with the increase of a quantity of the electrodeposited metal

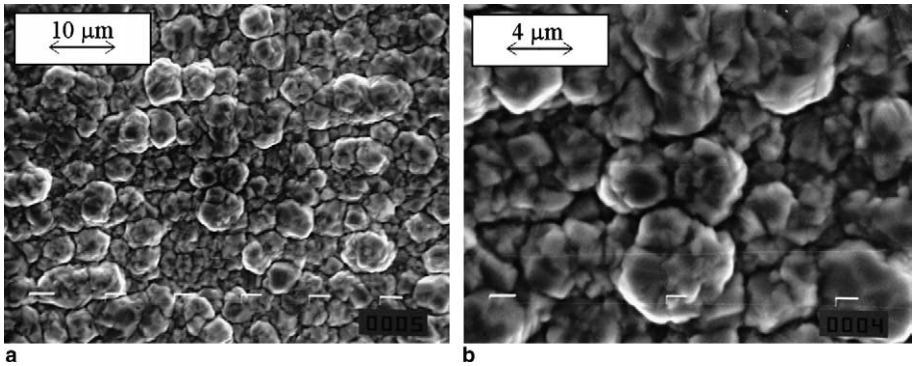

Fig. 5. Copper deposit obtained at overpotential of 550 mV. Quantity of electricity: 2.5 mAh cm^{-2}. Magnification: (a) 2000× and (b) 5000×.

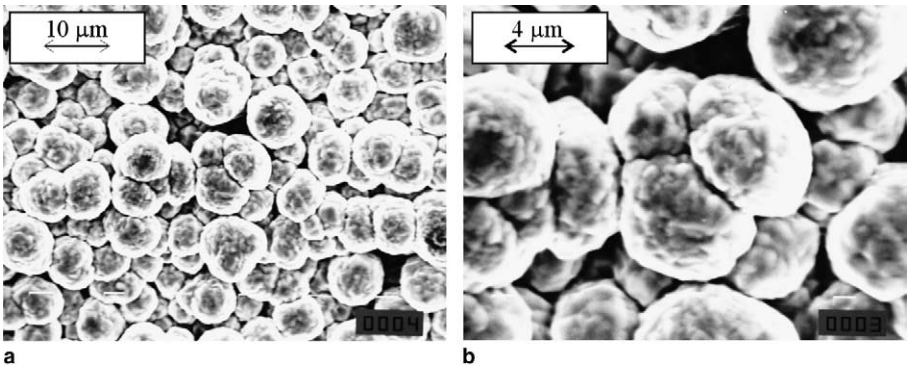

Fig. 6. Copper deposit obtained at overpotential of 550 mV. Quantity of electricity: 5.0 mAh cm^{-2}. Magnification: (a) 2000× and (b) 5000×.

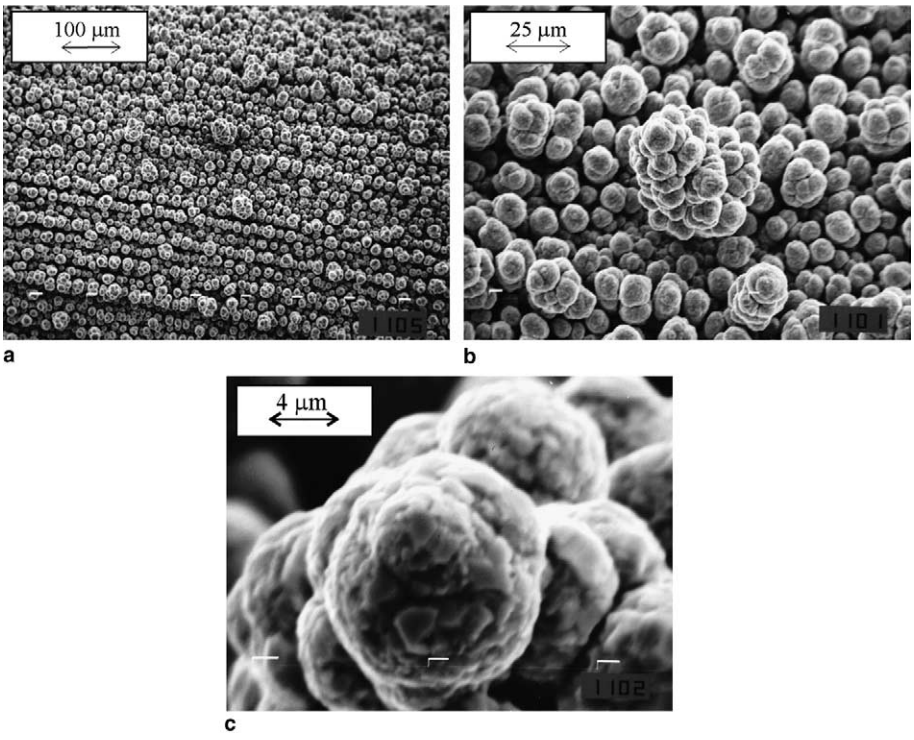

Fig. 7. Copper deposit obtained at overpotential of 550 mV. Quantity of electricity: 10 mAh cm^{-2}. Magnification: (a) 150×, (b) 750× and (c) 5000×.

(Fig. 13(a) and (b); the quantity of the electricity: 10 mAh cm^{-2}).

Fig. 14 shows the copper deposit obtained at an overpotential of 1000 mV with quantity of the electricity of 10.0 mAh cm^{-2}. At the first sight, the morphology of this copper deposit is similar to the morphology of copper deposit obtained at 800 mV, i.e., it is a honeycomb-like with a large craters due to the hydrogen codeposition. Meanwhile, the careful analysis of this copper deposit showed that there are some differences between morphologies of copper deposits obtained at overpotentials of 800 and 1000 mV, respectively. As a consequence of the intensive evolution of hydrogen at the overpotential of 1000 mV (the average current efficiency is approximately three times larger at the overpotential of 1000 mV than at the overpotential of 800 mV), the number of craters due to the attachment of the hydrogen bubbles is larger for the deposit obtained at the overpotential of 1000 mV (Fig. 14(a)) than for the copper deposit obtained at 800 mV with the same quantity of the electricity (Fig. 13(a)). Also, the electrodeposition at overpotential of 1000 mV led to a decrease of copper grain sizes with respect to the electrodeposition at 800 mV.

Finally, it can be noticed that the size of copper grains decreases with increasing deposition overpotentials from 550 to 1000 mV (Figs. 7(c), 13(b) and 14(b)). The increase of the dispersity of copper deposits with increasing deposition overpotentials is primarily due to the increase of the nucleation rate, as well as of the increase of the hydrogen evolution.

The obtained morphologies of copper deposits can be explained by the following consideration.

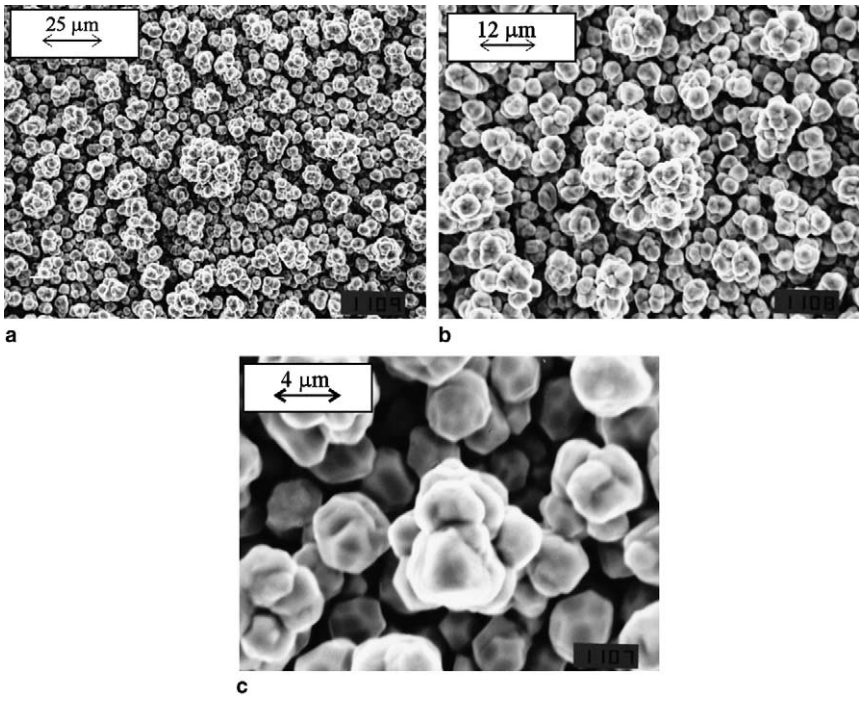

Fig. 8. Copper deposit obtained at overpotential of 700 mV. Quantity of electricity: 2.5 mAh cm^{-2}. Magnification: (a) 750×, (b) 1500× and (c) 5000×.

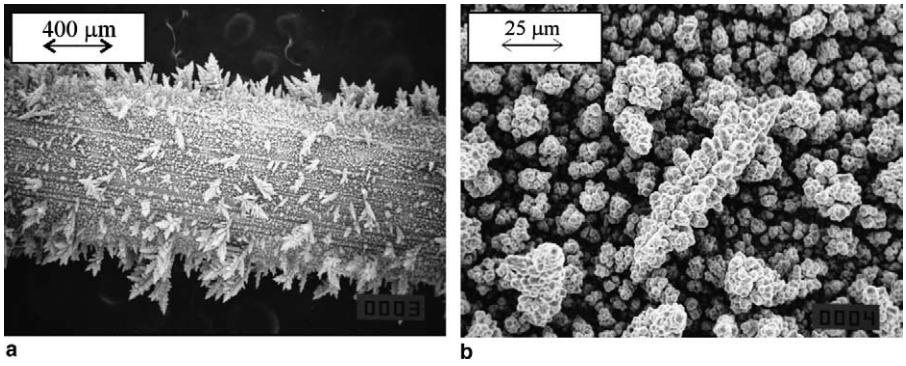

Fig. 9. Copper deposit obtained at overpotential of 700 mV. Quantity of electricity: 5.0 mAh cm^{-2}. Magnification: (a) 50× and (b) 750×.

Fig. 10. Copper deposit obtained at overpotential of 700 mV. Quantity of electricity: 10 mAh cm^{-2}. Magnification: 150×.

It is known that the hydrogen evolution effects onto the hydrodynamic conditions inside electrochemical cell [8–10]. The increase in hydrogen evolution rate leads to the decrease of the diffusion layer thickness and, hence, to the increase of limiting diffusion current density of electrode processes. It was shown [8] that if the rate of gas evolution at the electrode is larger than 100 cm^3/cm^2 min (>5 A/cm^2), the diffusion layer becomes only a few micrometers thick. It is also shown [8] that a coverage of an electrode surface with gas bubbles can be about 30%. If the thickness of the diffusion layer in conditions of natural convection is $\sim 5 \times 10^{-2}$ cm and in strongly stirred electrolyte $\sim 5 \times 10^{-3}$ cm [11], it is clear that gas evolution is the most effective way of the decrease of mass transport limitations for electrochemical processes in mixed activation–diffusion control.

The overpotential η and the current density i are related by

$$\eta = \frac{b_c}{2.3} \ln \frac{i}{i_o} + \frac{b_c}{2.3} \ln \frac{1}{1 - \frac{i}{i_L}}, \quad (1)$$

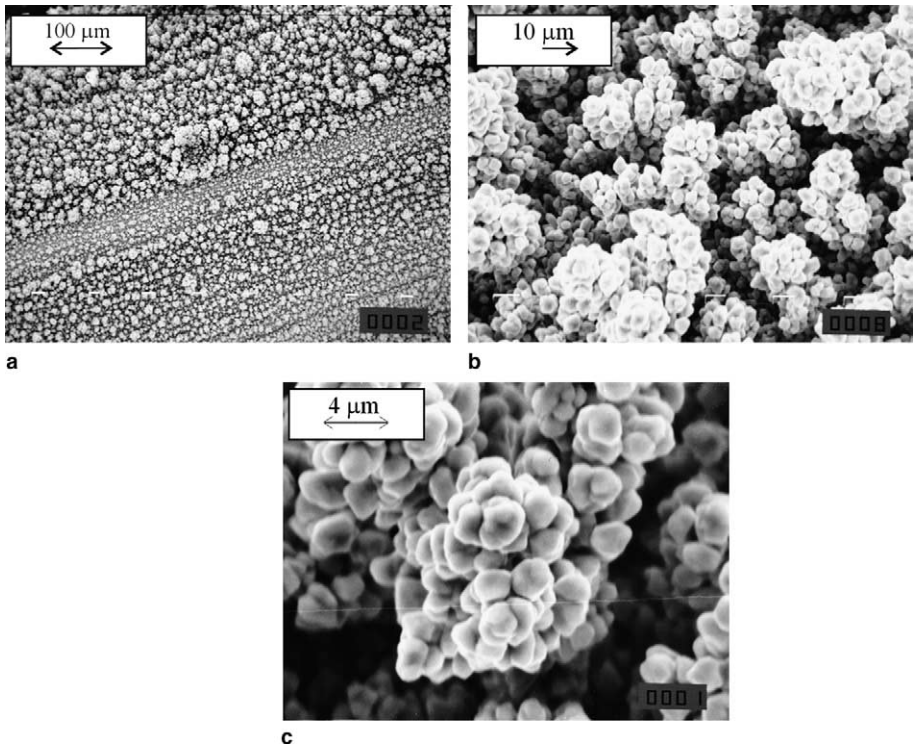

Fig. 11. Copper deposit obtained at overpotential of 800 mV. Quantity of electricity: 2.5 mAh cm^{-2}. Magnification: (a) 150×, (b) 2000× and (c) 5000×.

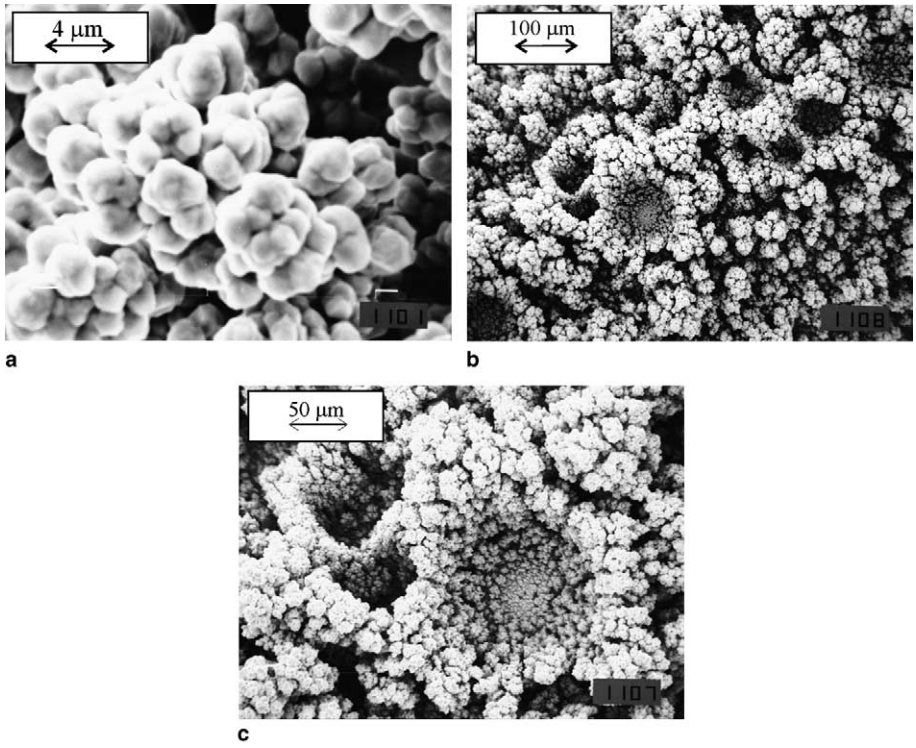

Fig. 12. Copper deposit obtained at overpotential of 800 mV. Quantity of electricity: 5.0 mAh cm^{-2}. Magnification: (a) 5000×, (b) 150× and (c) 350×.

where i_o, i_L and b_c are the exchange current density, the limiting diffusion current density and cathodic Tafel slope for electrochemical process in mixed activation–diffusion control [2]. The first term in Eq. (1) corresponds to the activation part of deposition overpotential and the second one is due to the mass transfer limitations. If one and the same process takes place under two different hydrodynamic conditions, characterised by two different values of the limiting

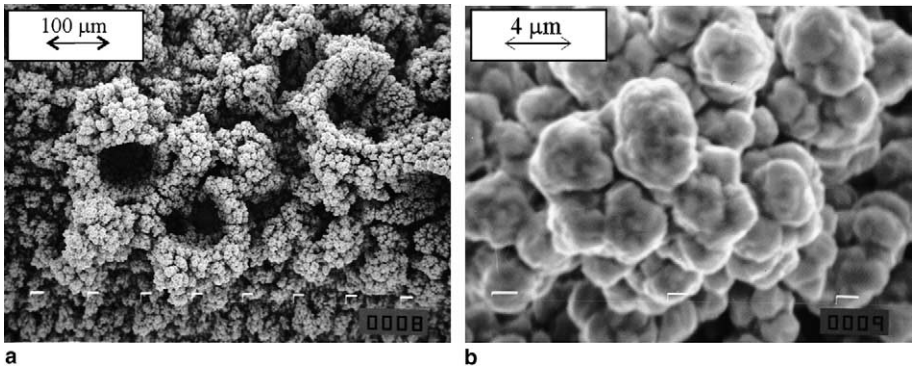

Fig. 13. Copper deposit obtained at overpotential of 800 mV. Quantity of electricity: 10 mAh cm^{-2}. Magnification: (a) 150× and (b) 5000×.

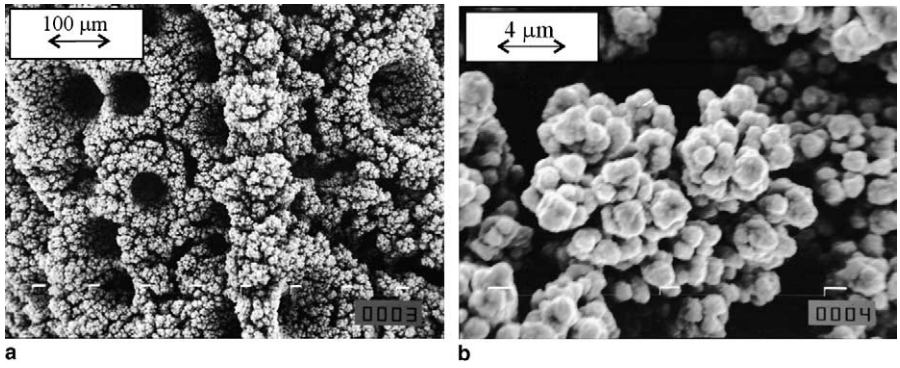

Fig. 14. Copper deposit obtained at overpotential of 1000 mV. Quantity of electricity: 10 mAh cm^{-2}. Magnification: (a) 150× and (b) 5000×.

diffusion current densities $i_{L,1}$ and $i_{L,2}$, the Eq. (1) can be rewritten in the forms:

$$\eta_1 = \frac{b_c}{2.3}\ln\frac{i_1}{i_o} + \frac{b_c}{2.3}\ln\frac{1}{1-\frac{i_1}{i_{L,1}}} \tag{2}$$

and

$$\eta_2 = \frac{b_c}{2.3}\ln\frac{i_2}{i_o} + \frac{b_c}{2.3}\ln\frac{1}{1-\frac{i_2}{i_{L,2}}}, \tag{3}$$

where η_1 and η_2 and i_1 and i_2 are the corresponding values of overpotentials and current densities.

The same degree of diffusion control is obtained if

$$\frac{i_1}{i_{L,1}} = \frac{i_2}{i_{L,2}} \tag{4}$$

or

$$i_2 = i_1\frac{i_{L,2}}{i_{L,1}} \tag{5}$$

and substitution of i_2 from Eq. (5) in Eq. (3) and further rearranging give

$$\eta_2 = \frac{b_c}{2.3}\ln\frac{i_1}{i_o} + \frac{b_c}{2.3}\ln\frac{1}{1-\frac{i_1}{i_{L,1}}} + \frac{b_c}{2.3}\ln\frac{i_{L,2}}{i_{L,1}} \tag{6}$$

and

if Eq. (2) is taken into account:

$$\eta_2 = \eta_1 + \frac{b_c}{2.3}\ln\frac{i_{L,2}}{i_{L,1}}. \tag{7}$$

Hence, if

$$i_{L,2} > i_{L,1} \tag{8}$$

in order to obtain the same degree of diffusion control in two hydrodynamic conditions, Eq. (7) must be satisfied, meaning that

$$\eta_2 > \eta_1. \tag{9}$$

The results obtained in this work can be then explained as follows. In the absence of hydrogen evolution, the diffusion layer is due to the natural convection and does not depend on the overpotential of electrodeposition. As excepted, for deposition times lower than the induction time for dendritic growth initiation, the same type of deposit at larger overpotential (Fig. 8) is obtained as at lower overpotential (Fig. 7), being somewhat different in grain sizes and particle shapes.

The intensive hydrogen evolution changes the hydrodynamic conditions and decreases the degree of diffusion control. Hence, Eq. (7) should be rewritten in the form:

$$\eta_1 = \eta_2 - \frac{b_c}{2.3}\ln\frac{i_{L,2}}{i_{L,1}}, \tag{10}$$

where η_1 becomes the effective overpotential, $\eta_1 = \eta_{eff}$, related to conditions of natural convection at which there is the same degree of diffusion control as at overpotential η_2 with the hydrogen codeposition. Hence, the dendritic growth can be delayed or completely avoided, as can be seen from Figs. 11–14, meaning that there is a really lower

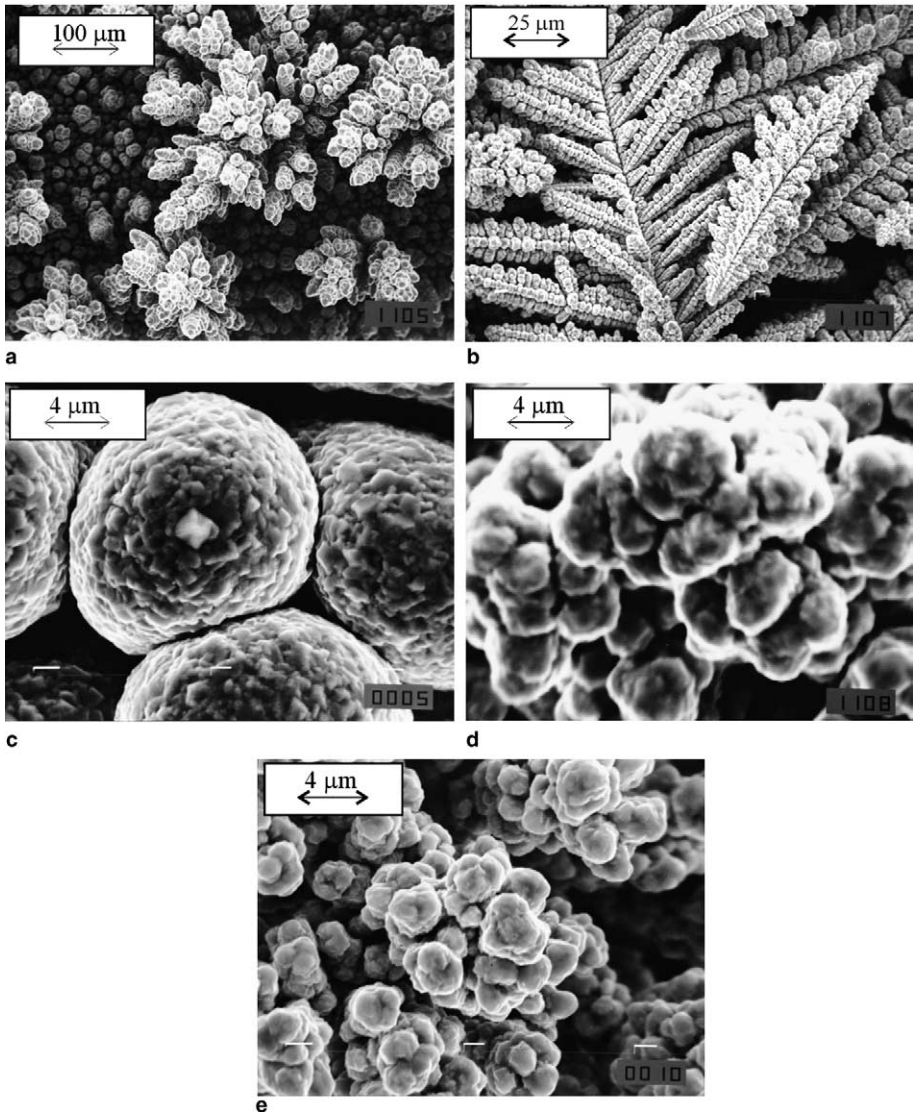

Fig. 15. Copper deposits obtained with the quantity of the electricity of 20 mAh cm^{-2} and at overpotentials of: (a) 550 mV; magnification: 200×, (b) 700 mV; 750×, (c) 450 mV; 5000×, (d) 800 mV; 5000× and (e) 1000 mV; 5000×.

degree of diffusion control at overpotentials of 800 and 1000 mV with the hydrogen codeposition than at overpotential of 700 mV, where the hydrogen codeposition is very small. On the other hand, the nucleation rate and the grain size depend on the overpotential, so the grain size is considerably decreased in electrodepositions at 800 and 1000 mV (Figs. 13 and 14(b)), relative to the electrodeposition at 550 mV (Fig. 7(c)). The holes between the agglomerates of grains are due to the large coverage with the hydrogen bubbles (Figs. 11–14).

Hence, on the basis of presented results, we can propose a concept of ''effective overpotential'' for a metal electrodeposition. This concept is proposed thanking to morphologies of copper deposits obtained at high deposition overpotentials (800 mV and more), where the hydrogen evolution takes place. These copper deposits are probably consequence of the stirring of electrolyte in the near-electrode layer by evolving hydrogen. This process leads to a decrease of the thickness of diffusion layer, and consequently, up to an increase of the limiting current density. According to Eq. (10), the increase of the limiting current density leads to a metal deposition at an overpotential which is effectively lower than the specified one. Then, the obtained morphologies of copper deposits become similar to ones obtained at some lower overpotential at which the hydrogen codeposition does not exist. In this case, it can be noticed that morphologies of copper deposits obtained at overpotentials of 800 and 1000 mV with the quantity of the electricity of 10 mAh cm^{-2} (Figs. 13(b) and 14(b)) were more similar to ones obtained at the overpotential of 550 mV (Fig. 7(c)) than at the overpotential of 700 mV (Fig. 10).

The better understanding of the concept ''effective overpotential'' can be realised by taking into account the fact that the time of dendritic growth initiation depends on used deposition overpotentials. Increasing deposition overpotentials

lead to decreasing times for the beginning of dendritic growth [7]. Observing deposits obtained at overpotentials belonging to the limiting diffusion current density plateau (550 and 700 mV) with the quantity of the electricity of 10 mAh cm^{-2}, one can notice that cauliflower forms are obtained at the overpotential of 550 mV (Fig. 7(b)), and dendritic forms at the overpotential of 700 mV (Fig. 10). Meanwhile, the electrodeposition with the quantity of the electricity of 20 mAh cm^{-2} leads to the formation of dendritic structure and at 550 mV (Fig. 15(a)). Copper dendrites remain a main characteristic of the electrodeposition at 700 mV (Fig. 15(b)). On the other hand, it can be shown that copper dendrites are not formed by the electrodeposition at lower overpotential (for example, at 450 mV where the hydrogen evolution was also zero) with the quantity of the electricity of 20 mAh cm^{-2} (Fig. 15(c)). The main forms of the copper deposit obtained at this overpotential are copper globules. Also, dendritic forms are not formed with the quantity of the electricity of 20 mAh cm^{-2} and during electrodepositions at overpotentials of 800 and 1000 mV, respectively (Fig. 15(d) and (e)). The agglomerates of copper particles remain main characteristics of deposits obtained at these overpotentials.

However, morphologies of copper deposits obtained at overpotentials of 800 and 1000 mV with the quantity of the electricity of 20 mAh cm^{-2} were similar to those obtained at lower overpotentials before the beginning of dendritic growth. The absence of copper dendrites at overpotentials of 800 and 1000 mV after the electrodeposition with 20.0 mAh cm^{-2}, as well as the similarity of the obtained morphologies of copper deposits with those obtained at lower overpotentials before dendritic growth initiation clearly indicates that there is really lower degree of diffusion control at these overpotentials than at overpotentials of 550 and 700 mV, respectively.

The concept of ''effective overpotential'' can be probably applied and in other cases, where there is a change of hydrodynamic conditions in the near-electrode layer. The change of hydrodynamic conditions, and consequently, of metal morphologies can be caused by stirring of plating solutions in ultrasonic field [12], in an imposed magnetic fields (magnetohydrodynamic effect – MHD effect) [13], as well as by stirring of solution by RDE (rotating disc electrode) [14].

This concept applied for the case of the effect of magnetic fields can be considered as follows.

When a parallely oriented magnetic field was applied during the nickel electrodeposition from a Watt solution with the addition of coumarin, the observed morphologies of nickel deposits were similar to those obtained without imposed magnetic fields at lower cathodic potential [13]. The morphology of nickel deposit obtained under a parallel oriented magnetic field of −1200 mV/SCE was similar to the morphology of nickel deposit obtained without an applied magnetic field at −1000 mV/SCE, while the nickel deposit obtained at −1300 mV/SCE (the magnetic field with a parallel orientation) was similar to the one obtained at −1200 mV/SCE without an applied magnetic field. In the case of copper electrodeposition, the morphology of copper deposit obtained at −500 mV/SCE under a parallel oriented magnetic field was cauliflower structure for the difference of the morphology of copper deposit obtained under the same condition but without an applied magnetic field which was a very developed dendritic structure [15]. The change of morphology of metal deposits can be ascribed to a forced convection of electrolytes due to the effect of a magnetic field on mass transport (MHD effect).

Similar effects can be observed during electrodeposition in an ultrasonic field [12]. Copper deposits obtained in an ultrasonic field were compact and more order structure in comparison with copper deposits obtained without an effect of ultrasonic fields.

Also, it was shown [16] that the major contribution to the mass transfer during electrodeposition of Cu/Ni–Cu multilayered structures by the single-bath method is made by the agitation of the near-electrode layer of electrolyte by evolving hydrogen.

In all cases, changes in morphologies of metal deposits are ascribed to the changes of hydrodynamic conditions, i.e., a decrease of diffusion layer thickness near to the electrode surface, and consequently, to an increase of the limiting current density. For example, it is adopted as a rule that under an imposed magnetic field the excess limiting current varies as $B^{1/3}c^{4/3}$, where B is magnetic flux density and c is a concentration of electroactive species [17].

However, morphologies of copper deposits observed at overpotentials of 800 and 1000 mV were similar to morphologies of copper and tin deposits which were recently reported [3]. Electrodes characterised by these morphologies can be successful used as electrodes for batteries, sensors and full cells. The reason for it is a very large surface area of these deposits caused by a very intensive the hydrogen evolution. As it was shown earlier, the electrodeposition at high overpotentials led to the decrease of grain sizes. For that reason, it can be supposed that the electrodepositions at very high overpotentials can be very successful tool for the formation of disperse, but adherent electrodes with grains approaching nano-sized dimensions. The development of these electrodes will be the subject in the future work.

4. Conclusions

Morphologies of copper deposits obtained at high electrodeposition overpotentials (450 mV and more) were analysed.

At overpotentials of 550 and 700 mV, dominant shapes of copper morphologies were dendritic forms. Copper dendrites are formed at 550 mV after the electrodeposition with the quantity of the electricity of 20.0 mAh cm^{-2}, while at overpotential of 700 mV copper dendrites are formed with the quantity of the electricity of 5.0 mAh cm^{-2}. At the overpotential of 450 mV, copper dendrites are not formed even with the quantity of the electricity of

20.0 mAh cm^{-2}. At this overpotential, dominant shapes of the copper morphology were copper globules.

At these overpotentials of the electrodeposition, the hydrogen evolution was zero (for overpotentials of 450 and 550 mV) or it was very small (for the overpotential of 700 mV).

At overpotentials of the electrodeposition (800 and 1000 mV), where the hydrogen evolution is noticeable, the dominant shapes of copper morphologies were a honeycomb-like with a large craters due to the hydrogen evolution. Agglomerates of copper grains are formed at these overpotentials, and it was shown that the increase of deposition overpotentials led to the decrease of copper grain sizes. At these overpotentials, copper dendrites are not formed.

The increase of dispersity of copper deposits was primarily due to the increase of deposition overpotential and, as consequence of the increase of overpotential, due to the increase of the hydrogen evolution rate.

On the basis of the obtained morphologies of copper deposits, the concept "effective overpotential" is proposed. According to this concept, when there is the change of hydrodynamic conditions in the plating solutions, the shape of obtained metal morphologies will be similar to the shape of metal morphologies obtained at some lower overpotential at which there is no the hydrodynamic effects. In this case, the change of hydrodynamic conditions which led to the change of morphologies of copper deposits was caused by the intensive stirring of the copper solution in the near-electrode layer by evolving hydrogen.

Acknowledgement

The work was supported by the Ministry of Science and Environmental Protection of the Republic of Serbia under the research project: "Deposition of ultrafine powders of metals and alloys and nanostructured surfaces by electrochemical techniques".

Appendix A

The determination of hydrogen current efficiency:

The average current efficiency of the hydrogen evolution was determined according to a literature procedure [18], modified for the case of a potentiostatic electrodeposition, in the following way.

The volume of evolved hydrogen was measured for different times of copper electrolysis. The volume of evolved hydrogen, $V(H_2)$ in a function of the time of electrolysis, t is given by

$$V_{H_2} = \mu(H_2) I_{H_2} t. \tag{11}$$

Then

$$I_{H_2} = \frac{V_{H_2}}{\mu(H_2) t}, \tag{12}$$

where $\mu(H_2)$ is given by

$$\mu(H_2) = \frac{V}{nF}(=)\frac{cm^3}{Ah}, \tag{13}$$

where V is molar volume of gas under normal condition (i.e., 22,400 cm^3).

The average current efficiency for the hydrogen evolution will be given by

$$\eta_{I,av}(H_2) = \frac{I_{H_2}}{I}, \tag{14}$$

where I is the overall current of copper electrodeposition.

In potentiostatic electrodeposition, the current of a metal electrodeposition is not constant, and it is a function of the time of electrolysis. In order to determine the current efficiency for the hydrogen evolution, for the overall current of a metal electrodeposition, I, we use the average current which is correlated with a current, I, and a quantity of electrodeposited metal, Q, by

$$I_{av} t = \int_0^t I \mathrm{d}t = Q, \tag{15}$$

i.e.,

$$I_{av} = \frac{\int_0^t I \mathrm{d}t}{t}. \tag{16}$$

According to Eqs. (12), (14) and (16), the average current efficiency for the hydrogen evolution in the function of a quantity of an electrodeposited metal, can be given by

$$\eta_{I,av}(H_2) = \frac{V_{H_2}}{\mu(H_2) \int_0^t I \mathrm{d}t}. \tag{17}$$

Then, for every 2 min, current I is measured (see Fig. 2), and graphical integration I–t is made.

(a) Example of the determination of the current efficiency of the hydrogen evolution.

- For $\eta = 800$ mV:

after $t = 22$ min ($t = 0.367$ h), current $I = 68.0$ mA ($I = 0.0680$ A).

$$\int_0^t I \mathrm{d}t = 0.0141 \text{ Ah}$$

and

$$\mu(H_2) = \frac{V}{nF} = \frac{22,400 \text{ cm}^3}{2 \times 26.8 \text{ Ah}} = 418 \frac{\text{cm}^3}{\text{Ah}}$$

The volume of the evolved hydrogen was $V = 0.675$ cm^3, and according to Eq. (17)

$$\eta_{I,av}(H_2) = \frac{0.675 \text{ cm}^3}{418 \frac{\text{cm}^3}{\text{Ah}} 0.0141} = 0.1144$$

or, in %:

$$\eta_{I,av}(H_2) = 11.44\%.$$

References

[1] K.I. Popov, N.V. Krstajić, M.I. Čekerevac, The mechanism of formation of coarse and disperse electrodeposits, in: R.E. White, B.E. Conway, J.O'M. Bockris (Eds.), Modern Aspects of Electrochemistry, Plenum Press, New York, 1996, pp. 261–311, references therein.

[2] K.I. Popov, S.S. Djokić, B.N. Grgur, Fundamental Aspects of Electrometallurgy, Kluwer Academic/Plenum Publishers, New York, 2002, references therein.
[3] H.-C. Shin, J. Dong, M. Liu, Adv. Mater. 15 (2003) 1610–1614.
[4] K.I. Popov, N.D. Nikolić, Z. Rakočević, J. Serb. Chem. Soc. 67 (2002) 635–638.
[5] K.I. Popov, N.D. Nikolić, Z. Rakočević, J. Serb. Chem. Soc. 67 (2002) 769–775.
[6] J.O'M. Bockris, Z. Nagy, D. Dražić, J. Electrochem. Soc. 120 (1973) 30–41.
[7] K.I. Popov, M.D. Maksimović, J.D. Trnjančev, M.G. Pavlović, J. Appl. Electrochem. 11 (1981) 239–246.
[8] N. Ibl, Chem. Ing. Tech. 33 (1961) 69–74.
[9] N. Ibl, Chem. Ing. Tech. 35 (1963) 353–361.
[10] L.J. Jenssen, J.G. Hoogland, Electrochim. Acta 15 (1970) 1013–1023.
[11] J.O'M. Bockris, A.K.N. Reddy, M. Gamboa-Aldeco, Modern Electrochemistry 2A – Fundamentals of Electrodics, second ed., KluwerAcademic/Plenum Publishers, New York, 2000.
[12] L. Martins, J.I. Martins, A.S. Romeira, M.E. Costa, J. Costa, M. Bazzaoui, Mater. Sci. Forum 455–456 (2004) 844–848.
[13] N.D. Nikolić, H. Wang, H. Cheng, C. Guerrero, E.V. Ponizovskaya, G. Pan, N. Garcia, J. Electrochem. Soc. 151 (2004) C577–C584.
[14] M.G. Pavlović, Š. Kindlova, I. Roušar, Electrochim. Acta 37 (1992) 23–27.
[15] N.D. Nikolić in preparation.
[16] S.N. Ovchinikova, N.P. Poddubnyi, A.I. Maslii, V.V. Boldyrev, W. Schwarzacher, Russ. J. Electrochem. 38 (2002) 1210–1215.
[17] R. Aogaki, K. Fueki, T. Mukaibo, Denki Kagaku 43 (1975) 509–514.
[18] M.G. Pavlović, N.D. Nikolić, K.I. Popov, J. Serb. Chem. Soc. 68 (2003) 649–656.